Virology 385 (2009) 313–322

Contents lists available at ScienceDirect

Virology

journal homepage: www.elsevier.com/locate/yviro

Microtubule-dependent and microtubule-independent steps in Crimean-Congo hemorrhagic fever virus replication cycle

Melinda Simon [a,b,*], Cecilia Johansson [a,b], Åke Lundkvist [a], Ali Mirazimi [a,b]

[a] Department of Microbiology, Tumor and Cell Biology, Karolinska Institutet, S-171 77 Stockholm, Sweden
[b] Centre for Microbiological Preparedness, Swedish Institute for Infectious Disease Control, S-171 82 Stockholm, Sweden

ARTICLE INFO

Article history:
Received 21 July 2008
Returned to author for revision
25 August 2008
Accepted 5 November 2008
Available online 15 January 2009

Keywords:
CCHFV
Nairovirus
Nocodazole
Paclitaxel
Microtubules

ABSTRACT

Following binding and entry many viruses exploit the host cell cytoskeleton to ensure intracellular transport, assembly or egress. For Crimean-Congo hemorrhagic fever virus (CCHFV), the causative agent of a severe hemorrhagic disease, virus–host interactions are poorly investigated. In this study we demonstrated that drug-induced suppression of microtubule dynamics and especially microtubule disassembly, impaired CCHFV biogenesis. Our results showed that intact microtubules were required early during virus internalization, and late, during virus assembly and egress. Furthermore, disruption of microtubules resulted in reduced levels of viral RNA while preservation of microtubule dynamics was most important during viral egress. Finally, although CCHFV proteins were redistributed in drug-treated cells, the glycoprotein remained associated with the Golgi apparatus, the organelle of virus budding. Taken together, our results suggest that manipulation of microtubules affects CCHFV entry, replication, assembly and egress.

Introduction

Crimean-Congo hemorrhagic fever virus (CCHFV) is the causative agent of a serious human infection and has a reported case fatality ranging between 3 and 30% (Ergonul, 2006; Whitehouse, 2004). The virus belongs to the *Nairovirus* genus, family *Bunyaviridae*, and circulates in nature in an enzootic tick–vertebrate–tick cycle (Schmaljohn and Nichol, 2007). Infected animals are usually asymptomatic while in humans, the disease is manifested by symptoms such as fever, prostration and hemorrhage (Swanepoel et al., 1987).

To date, CCHFV has been isolated from more than 30 different tick species throughout the world with *Hyalomma* ticks as the principal vector (Schmaljohn and Nichol, 2007). Recently, tick-borne diseases has attracted focus since prevailing climate changes has been shown to facilitate reproduction of tick populations and consequently increase the incidence of tick-borne infections (Gubler et al., 2001). Dissemination of CCHFV can also occur via birds that are refractory to CCHFV infection but may carry the infected ticks over long distances (Zeller et al., 1994). The molecular mechanism underlying CCHFV pathogenesis, entry route and intracellular trafficking are currently poorly understood and research is further hampered by the requirement of specialized laboratories, limited clinical facilities and the lack of animal models.

Numerous studies have demonstrated the frequent employment of host cell cytoskeleton in viral trafficking, assembly or exit (Dohner and Sodeik, 2005; Jouvenet et al., 2004; Lakadamyali et al., 2003; McDonald et al., 2002; Newsome et al., 2004; Pelkmans et al., 2001; Rietdorf et al., 2001; Sodeik et al., 1997; Suomalainen et al., 1999; Yonezawa et al., 2005). The actin filaments are primarily found directly beneath the plasma membrane while microtubules are present throughout the cell. Therefore, for viruses that fuse with the plasma membrane (HIV, herpes simplex virus), the dense actin cortex provides a barrier during viral entry (Luby-Phelps, 2000). Most viruses however, enter their host cells via the endocytic route and bypass the actin barrier by traversing inside vesicles. Subsequent intracellular transport occurs either by the direct interaction of the virus with tubulins or via the endogenous endocytic pathway (Dohner and Sodeik, 2005; Smith and Enquist, 2002). While the use of microtubules in intracellular trafficking is well characterized, less is known about the role of microtubules in viral transcription and replication. There are however a few studies demonstrating a role for both actin filaments and microtubules in successful viral RNA expression (De et al., 1993; Gupta et al., 1998; Kuhn et al., 2005; Mallardo et al., 2001; Naghavi et al., 2007). Finally, to complete the viral life cycle, several viruses interfere with actin filaments or microtubules before exit occurs via exocytosis or cell lysis (Igakura et al., 2003; Jouvenet et al., 2004; Jouvenet and Wileman, 2005; Ploubidou et al., 2000; Simpson-Holley et al., 2002; Smith and Helenius, 2004; Smith and Enquist, 2002).

* Corresponding author. Swedish Institute for Infectious Disease Control, S-171 82 Stockholm, Sweden. Fax: +46 8 30 79 57.
E-mail addresses: melinda.simon@smi.ki.se (M. Simon), cecilia.johansson@smi.ki.se (C. Johansson), ake.lundkvist@smi.ki.se (Å. Lundkvist), ali.mirazimi@smi.ki.se (A. Mirazimi).

0042-6822/$ – see front matter © 2008 Elsevier Inc. All rights reserved.
doi:10.1016/j.virol.2008.11.020

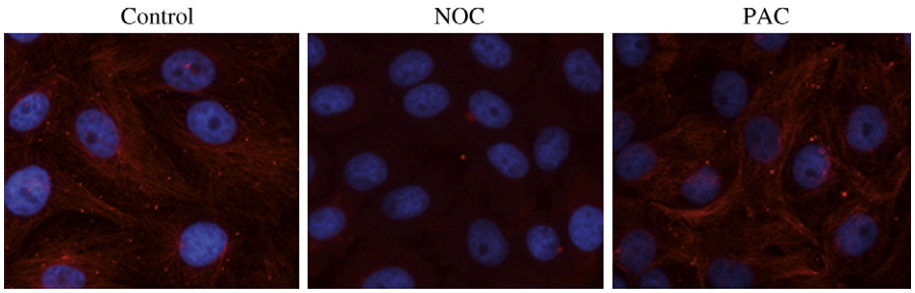

Fig. 1. Microtubule depolymerization and stabilization in response to NOC and PAC, respectively. Vero E6 cells were incubated in medium, 5 μM NOC or 20 μM PAC for 30 min before fixed and stained for α-tubulin. Nocodazole (NOC), paclitaxel (PAC).

The replication cycle of members of the *Bunyaviridae* family has been demonstrated to occur in the cytoplasm (Schmaljohn and Nichol, 2007). Only a few publications has so far studied the employment of host cell cytoskeleton in the life cycle of members within the *Bunyaviridae* (Andersson et al., 2004; Banes and Coleman, 1980; Ramanathan et al., 2007; Ramanathan and Jonsson, 2008; Ravkov et al., 1998).

Recently, it was shown that an intact cell cytoskeleton is critical for the efficient replication of several *Hantaviruses* (Ramanathan et al., 2007; Ramanathan and Jonsson, 2008). With regard to CCHFV, we have previously shown that actin is important for the perinuclear localization of CCHFV nucleocapsid protein (NP) and that actin and NP co-immunoprecipitates (Andersson et al., 2004). In addition, progeny virus titers are significantly reduced when actin is disrupted (Andersson et al., 2004). The role of microtubules however, has to our knowledge not been investigated for CCHFV or any other members of the Nairovirus genera.

In this study, we have examined the effects of two drugs that either depolymerize or stabilize microtubules, in the life cycle of CCHFV. We found that virus internalization was dependent on intact microtubules, and when internalization was allowed in the absence of drugs, primary transcription was equally efficient in drug-treated as in control cells. Depolymerization of microtubules was also inhibitory for the expression of CCHFV RNA and consequently to progeny virus production. Finally, efficient virus assembly was dependent on intact microtubules while CCHFV egress was dependent on both intact and dynamic microtubules.

Results

Manipulation of microtubules is fast, reversible and does not affect cellular viability

First, we investigated the kinetics of microtubule depolymerization and stabilization in response to nocodazole (NOC) or paclitaxel (PAC) treatment, respectively. Staining against α-tubulins showed that depolymerization and stabilization occurred within 30 min in response to 5 μM NOC or 20 μM PAC, respectively (Fig. 1). In addition, microtubule structure was restored within 30 min after NOC or PAC washout (data not shown). Moreover, lactate dehydrogenase (LDH)-assay showed that cell viability was not compromised despite treatment of cells with NOC or PAC for as long as 24 h (data not shown).

Perturbation of microtubules reduces CCHF progeny virus titers

To analyze the effects of NOC or PAC on total progeny virus production, cells were treated with NOC or PAC before and throughout infection for 24 h before cells and supernatants were collected and titrated for progeny virus assessment (Fig. 2B, −1 h). Results showed a significant ($p<0.001$) decrease in progeny virus titers for both NOC and PAC treated cells. Alternatively, cells were first infected and treated with NOC or PAC six to 24 h after infection (Fig. 2B, 6 hpi). Again, progeny virus titers were significantly ($p<0.001$) lower in NOC and PAC treated cells compared to control. Moreover, we found that progeny virus titers were significantly ($p<0.001$) lower in samples treated with NOC or PAC before and throughout infection (−1h) compared to cells that were treated 6 h after infection (6 hpi). These data suggest an important role of microtubules in the life cycle of CCHFV. Moreover, our results also suggest that part of the microtubule mediated inhibition occurs during the first 6 h of infection.

CCHFV infection begins with positive sense RNA synthesis

Observing that microtubule integrity is important in CCHFV biogenesis, we were interested to see in what step/s of the viral life cycle microtubules were necessary. Because there is to date little known about the kinetics of CCHFV RNA expression and synthesis, we

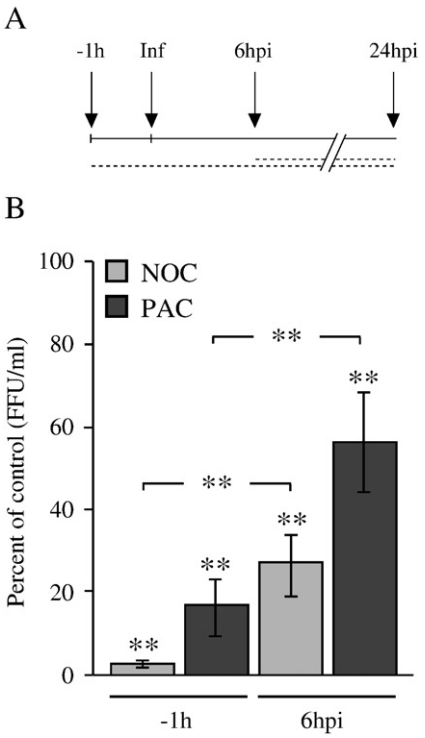

Fig. 2. Production of CCHF progeny virus is reduced in response to microtubule perturbations. Schematic illustration of drug treatments: dashed lines demonstrate the start, duration and stop of NOC or PAC treatments (A). Vero E6 cells were pretreated with NOC or PAC and infected in the presence of drugs for 24 h (−1h). Alternatively, cells were first infected and 6 h later treated with NOC or PAC (6 hpi). At the end of the infection total progeny virus (extracellular and intracellular) was collected and titrated for the assessment of progeny virus titers. Progeny virus in control cells corresponded to 1×10^7 FFU/ml. Presented data shows the average and standard deviations of three separate experiments. Significance is illustrated with $p<0.001$ (**). Nocodazole (NOC), paclitaxel (PAC).

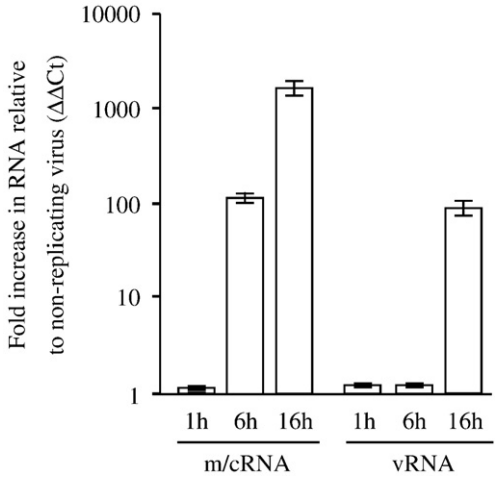

Fig. 3. CCHFV RNA synthesis over time. Vero E6 cells were infected with CCHFV for one, six or 16 h. At the end of each incubation period cells were harvested, RNA was purified and analyzed. Positive (messenger (m)/complementary (c)) and negative (viral (v)) CCHFV RNA was quantified relative to bound non-replicating input virus that was set to 1. Data represent the averages and standard errors of experiments performed in triplicates.

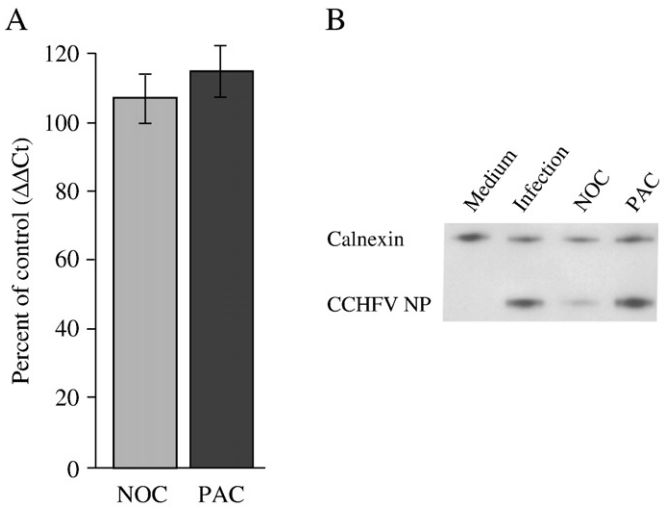

Fig. 4. CCHFV internalization requires intact microtubules. To determine CCHFV binding to cells in response to drugs, cells were pretreated with NOC or PAC followed by virus adsorption for 1 h at 4 °C before cells were harvested (A). Total RNA was purified and quantified relative to control. To assess internalization, cells were pretreated similar to the binding assay above before CCHFV internalization was allowed to proceed for 1 h at 37 °C (B). At the end of the incubation period, cells were rinsed in low pH buffer to inactivate non-internalized virus particles. Efficient internalization was determined 24 h later by analyzing viral protein (NP) expression. Presented data shows the average and standard deviations of three separate experiments (a). Nocodazole (NOC), paclitaxel (PAC), nucleocapsid protein (NP).

investigated CCHFV RNA expression over time first. Vero E6 cells were infected and maintained for one, six or 16 h before cells were harvested and CCHFV RNA expression was analyzed (Fig. 3). The increase in RNA levels over time was determined relative to bound, non-replicating virus. We found that during the first 6 h of infection CCHFV RNA expression increased and comprised mainly of positive sense RNA (mRNA and possibly complementary RNA (cRNA)). In contrast, negative sense RNA (vRNA) remained constant within this time period. Since vRNA levels increased by 16 h post infection (hpi), it seems that initiation of replication and therefore vRNA synthesis occurred sometimes between six and 16 hpi.

Microtubule depolymerization impair CCHFV internalization

Because drug treatment before and during the first 6 h of infection impaired CCHFV biogenesis to a greater extent (Fig. 2), we performed a number of experiments to investigate the role of microtubules in early CCHFV infection specifically.

To investigate binding of CCHFV to Vero E6 cells, cells were pretreated with NOC or PAC before virus was adsorbed to cells for 1 h at 4 °C (Fig. 4A). Thereafter, cells were rinsed and harvested before RNA was purified and quantified. Results showed that CCHFV RNA levels were similar in all three, control, NOC and PAC treated cells, suggesting that binding of CCHFV to its host cells was not impaired by depolymerization or stabilization of microtubules.

To determine internalization in the presence of NOC or PAC, cells were pretreated with the drugs and viral entry was allowed to occur for 1 h at 37 °C (Fig. 4B). At the end of the incubation, cells were rinsed in low pH buffer to inactivate non-internalized virions. Successful infection was assayed 24 h later by western blot. Our results showed a clear reduction in CCHFV nucleocapsid protein (NP) levels in NOC but not PAC treated cells, suggesting that intact microtubules were required in the internalization of CCHFV.

Microtubule perturbation does not interfere with primary transcription

Since internalization was affected by microtubule depolymerization (Fig. 4B), we were not surprised to see that RNA levels, quantified 6 hpi, were significantly ($p<0.001$) lower in cells where NOC had been added before infection (−1h) and maintained until harvest (Fig. 5B). Surprisingly, we also observed a significant ($p<0.05$) decrease in RNA levels in response to PAC treatment (Fig. 5B), suggesting that some dynamic property of microtubules need to be maintained in the early events of CCHFV infection. However, if CCHFV internalization occurred in the absence of drugs, with drugs present one to 6 hpi, CCHFV RNA expression was similar to control in NOC and

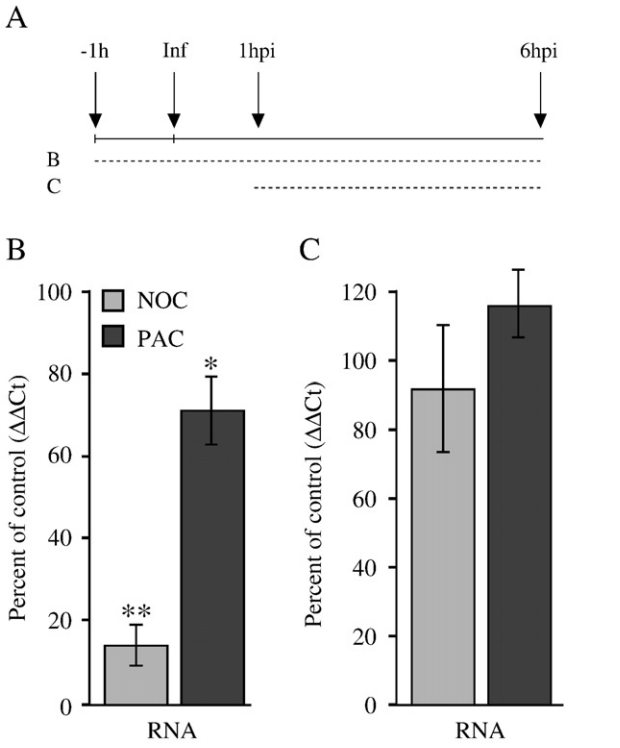

Fig. 5. Microtubule integrity is not important for CCHFV primary transcription. Schematic illustration of drug treatments: dashed lines demonstrate the start, duration and stop of NOC or PAC treatments (A). Vero E6 cells were NOC or PAC treated before and during infection for 6 h before cells were harvested, and total RNA was purified and quantified (B, −1h). Alternatively, cells were drug treated 1 hpi and maintained in the presence of drugs for 6 h before cells were harvested and total RNA was quantified (C). Results show the average and standard deviations of three separate experiments. Significance is illustrated with $p<0.05$ (*) or $p<0.001$ (**). Nocodazole (NOC), paclitaxel (PAC).

PAC treated cells. These results suggest that microtubule integrity and especially intact microtubules are important for CCHFV early events. Moreover, our results also indicate that following the first hour after infection, CCHFV transcription is not dependent on maintained microtubule integrity.

Prolonged depolymerization of microtubules reduces CCHF progeny virus and RNA levels

To address the effects of perturbed microtubules on CCHFV replication, Vero E6 cells were treated with NOC or PAC one to 16 hpi before cells were harvested (Figs. 6A–C). Drugs were added 1 hpi to elude the negative effects of microtubule manipulation early in infection (Fig. 4B) and 16-hour infections were chosen for harvest in order to minimize contribution of more than one round of CCHFV replication cycle. We found that drug treatment one to 16 hpi decreased intracellular progeny virus and CCHFV RNA levels in depolymerized but not stabilized cells (Fig. 6B). NOC treatment resulted in a significant ($p<0.001$) reduction of cell-associated progeny virus while virus titers from PAC treated cells were similar to control (Fig. 6B). Consistent with these results, quantification of CCHFV RNA revealed an approximately two-fold and significant ($p<0.05$) decrease in NOC but not PAC treated cells (Fig. 6C). Instead, RNA levels were significantly higher ($p<0.05$) in PAC treated cells compared to control (Fig. 6C). To investigate whether the increase in RNA levels were in response to PAC treatment and microtubule stabilization specifically, cells were first PAC treated similar to 6A and B. Sixteen hpi PAC was rinsed away and cells were maintained for one or 2 h in the absence of the drug before cells were harvested and RNA was analyzed (Fig. 6D). Our results showed that CCHFV RNA levels decreased with time to drug washout, suggesting that microtubule stabilization enhanced RNA synthesis. Taken together, our results indicate an important role for intact microtubules but not their dynamic turnover in the replication process of CCHFV.

Microtubule depolymerization and stabilization alter the intracellular distribution of CCHFV nucleocapsid protein and the glycoprotein G_N

To study the intracellular distribution of CCHFV NP and the glycoprotein G_N in response to microtubule depolymerization and stabilization, Vero E6 cells were treated with NOC or PAC and 24 hpi cells were fixed and stained for α–tubulins and NP or G_N. In control cells, NP localized to a number of sites close to the cell nucleus while G_N was mainly seen as a single perinuclear staining (Fig. 7A, left panel). When microtubules were depolymerized with NOC, NP redistributed to peripheral sites and partly maintained its perinuclear staining while G_N was completely dispersed within these cells (Fig 7A, middle panel). In response to PAC, NP staining was similar to control while G_N dislocated from perinuclear to more peripheral, yet concentrated sites within cells (Fig. 7A, right panel).

Since CCHFV assembly takes place in the Golgi apparatus (Schmaljohn and Nichol, 2007), perturbation of Golgi structure or function could result in poor assembly and reduced progeny virus titers. Therefore, we investigated the drug-mediated effects on the Golgi apparatus and the redistribution of CCHFV proteins by performing colocalization analysis of CCHFV NP and G_N with GM130 (cis-Golgi marker) (Fig. 7B). In control cells we found that NP localized close to GM130 but without any detectable colocalization (Fig. 7B, upper left panel). In contrast, we observed a distinct association between G_N and GM130 (Fig. 7B, lower left panel). Consistent with previous results, Golgi was completely fragmented in response to NOC (Fig. 7B, middle panel) while PAC treatment displaced Golgi from perinuclear to peripheral sites within cells (Fig. 7B, right panel). Despite Golgi fragmentation and displacement, association of G_N with

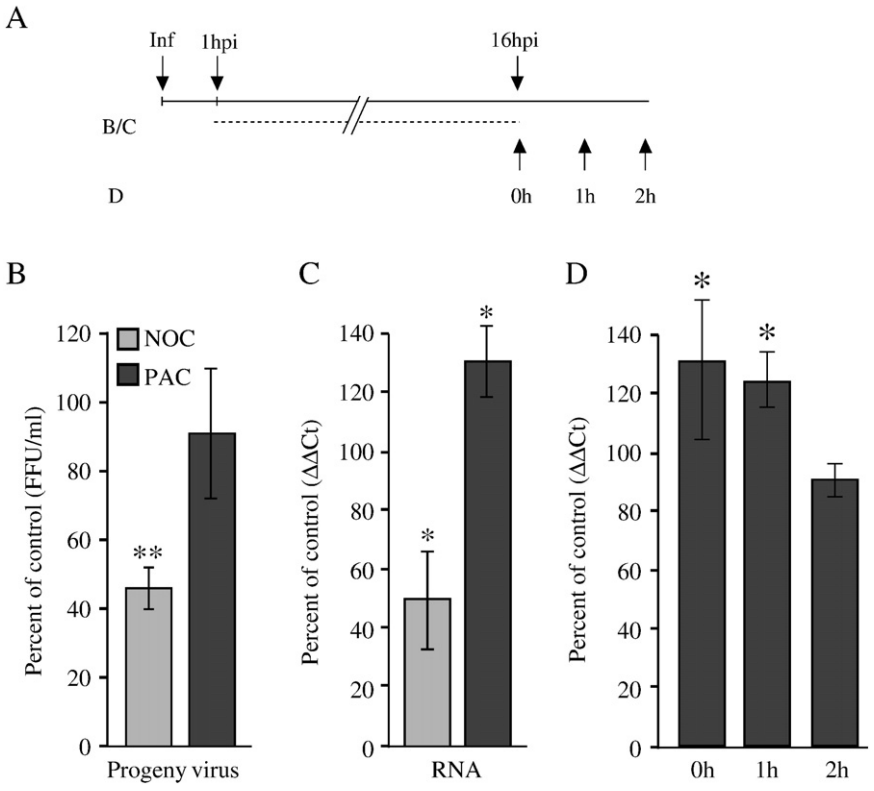

Fig. 6. Depolymerization of microtubules decreases CCHFV RNA and progeny virus levels. Schematic illustration of drug treatments: dashed lines demonstrate the start, duration and stop of NOC or PAC treatments (A). Vero E6 cells were drug treated one to 16 hpi before cell-associated progeny virus was harvested and titrated (B). In parallel, cells were also harvested for the assessment of CCHFV total RNA synthesis (C). To investigate the role of PAC on total RNA synthesis, cells were first drug treated one to 16 hpi. Thereafter cells were rinsed and maintained for one or 2 h in the absence of PAC before cells were harvested and RNA was analyzed (D). Progeny virus in control cells corresponded to $1x10^5$ FFU/ml. Results show the average and standard deviations of three separate experiments. Significance is illustrated with $p<0.05$ (*) or $p<0.001$ (**). Nocodazole (NOC), paclitaxel (PAC).

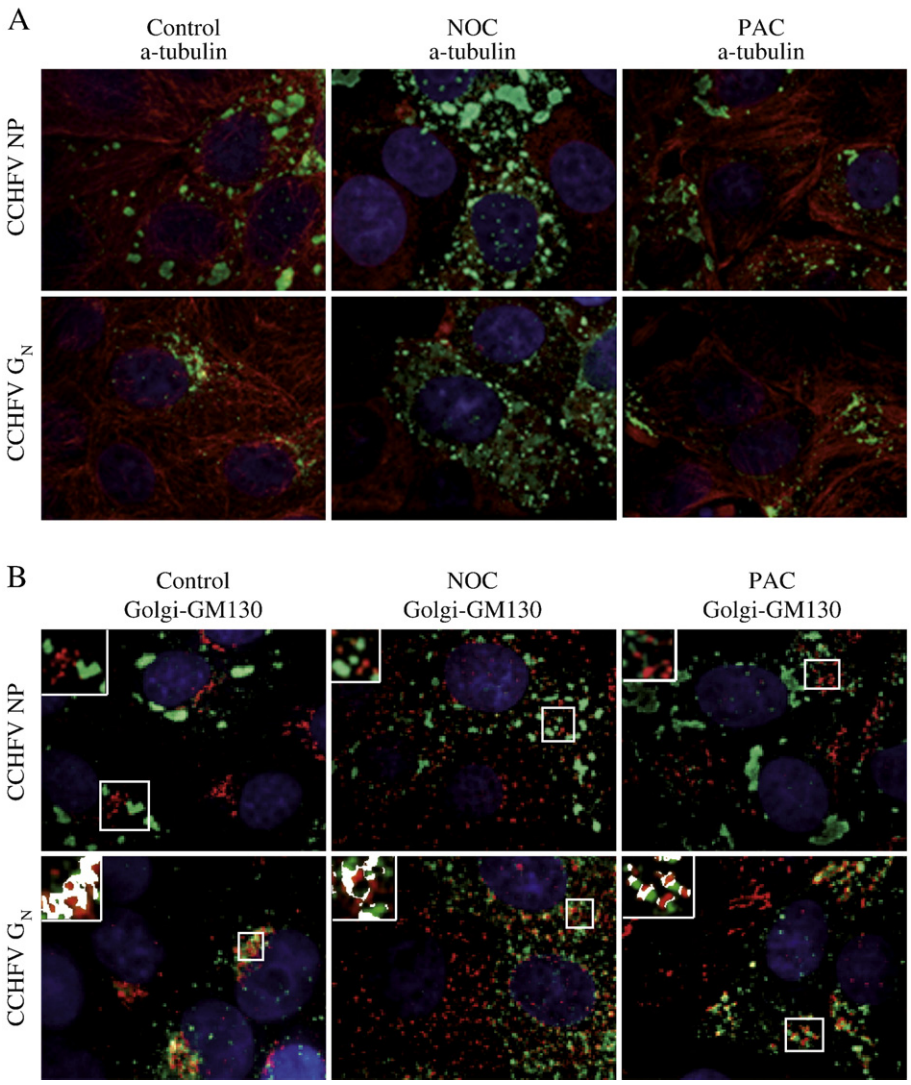

Fig. 7. Pertubation of microtubules redistributes CCHFV proteins. Intracellular localization of CCHFV nucleocapsid protein (NP) and the glycoprotein G_N was investigated in response to NOC or PAC treatment. Vero E6 cells were infected and treated with NOC or PAC between six and 24 hpi before cells were fixed and stained against NP, G_N and α-tubulins (A) or NP, G_N and GM130 (a cis-Golgi marker) (B). Pictures were analyzed by confocal microscopy and representative images are shown for each drug and control treatments. Association of G_N with GM130 is demonstrated in the insets, highlighted in white. Nocodazole (NOC), paclitaxel (PAC).

GM130 was still substantial (Fig. 6B, lower panel). Similar to control cells, NP showed little or no association with GM130 regardless of drug treatment (Fig. 6B, upper panel). These data show that although Golgi was fragmented or displaced in response to drug treatments, association between G_N and GM130 was largely maintained. This suggests a partly sustained pathway of CCHFV biosynthesis through the Golgi apparatus, a prerequisite for virus assembly and maturation.

Microtubule depolymerization or stabilization inhibits CCHFV egress

To investigate the engagement of microtubules in CCHFV egress, Vero E6 cells were rinsed free of existing progeny virus at 24 hpi and treated with NOC or PAC for 1 h (Fig. 8B). At the end of drug treatment, extracellular progeny virus was collected and titrated. Results showed that progeny virus titers decreased significantly ($p<0.001$) for NOC and PAC treated cells compared to control (Fig. 8B). To assess the effects of drug reversion on extracellular progeny virus, the drug treated cells were rinsed free of NOC or PAC and maintained for an additional hour (Fig. 8B). As a consequence of regained microtubule function, harvested progeny virus titers were restored and did not differ significantly from control (Fig. 8B). Because poor virus release could be due to poor intracellular virus assembly, we investigated the cell-associated progeny virus levels. Cells were treated as above and intracellular progeny virus was collected 1 h after drug treatment and 1 h after drug washout (Fig. 8C). We observed a significant decrease in progeny virus levels in response to NOC and a significant increase in progeny virus levels in response to PAC, suggesting that NOC impairs virus assembly while PAC causes intracellular virus accumulation. To determine the net effect of progeny virus formation, we summed the intracellular and extracellular progeny viruses in each mock or drug treated samples. In NOC treated cells progeny virus levels remained significantly ($p<0.05$) lower, suggesting that there was less progeny virus formation overall (data not shown). In agreement with previous results (Fig. 6B), total progeny virus titers in PAC treated cells were similar to control levels (data not shown) and suggest that stabilized microtubules mainly impair CCHFV egress. Taken together, our results suggest that microtubules are engaged in CCHFV egress and when microtubules are manipulated, viral egress is impeded. Moreover, intact microtubules are also important for efficient virus assembly.

Discussion

In this study we have investigated the role of microtubules in the replication cycle of CCHFV. We found that internalization was dependent

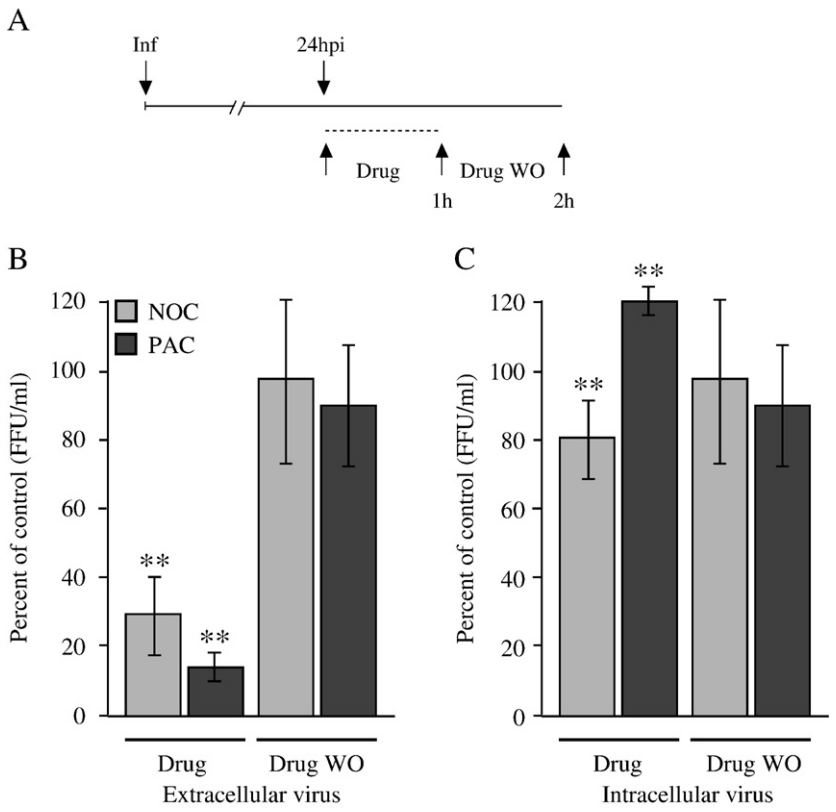

Fig. 8. Perturbation of microtubules inhibits CCHFV egress. Schematic illustration of drug treatments: dashed lines demonstrate the start, duration and stop of NOC or PAC treatments (A). Vero E6 cells were infected and treated with NOC or PAC between 25 and 26 hpi before extracellular progeny virus was collected (B). To assess reversion of drugs, cells were rinsed free of drugs and maintained for 1 h before supernatants were harvested and titrated (B, washout (WO)). In parallel, progeny virus was also harvested from the intracellular compartment (C). Presented data shows the average and standard deviations of three separate experiments. Significance is illustrated with $p<0.001$ (**). Nocodazole (NOC), paclitaxel (PAC).

on intact microtubules whereas primary transcription was independent of microtubule integrity. In response to depolymerization of microtubules (DM), CCHFV RNA and progeny virus levels decreased while stabilization of microtubules (SM) and DM impaired viral egress. Thus, the data presented here reveal some new roles of microtubules in the replication cycle of viruses that do not replicate in the nucleus.

Although the entry mechanism of CCHFV is not known, Hantaan virus, (genus *Hantavirus*, family *Bunyaviridae*) has been shown to use receptor-dependent clathrin-mediated endocytosis (Gavrilovskaya et al., 1998; Jin et al., 2002). The entry mechanism of CCHFV has not been addressed in this study; nonetheless, we show that binding is independent of microtubules. Indeed, these findings are in line with previous reports which demonstrate that microtubules are dispensable for viral binding to the host cell (Chu and Ng, 2004; Dohner et al., 2002; Funk et al., 2004; Lakadamyali et al., 2003; Suikkanen et al., 2003) (Fig. 3). Once inside the cell, CCHFV needs to be transported to the appropriate target sites before transcription and replication can be initiated.

In this study we demonstrated that DM resulted in reduced CCHFV early RNA synthesis (Fig. 5B). Closer analysis revealed that intact microtubules were required already at the level of virus internalization (Fig. 4B). The fact that SM reduced CCHFV early RNA synthesis (Fig. 5B) without the expected reduction in virus internalization *per se* (Fig. 4B) suggests that microtubules may be engaged in post-internalization steps as well. We therefore hypothesize that the first hour following CCHFV infection reflects the time needed for CCHFV to become internalized and move along microtubules to reach the site of viral transcription.

In this study we have also showed, for the first time, that early infection (up to 6 hpi) consisted of positive sense RNA (m/cRNA) synthesis while no increase could be detected in genomic, negative RNA (vRNA) (Fig. 3). Consequently, early CCHFV infection most likely represents viral transcription. Our results also indicate that subsequent to early events following the first hour post infection, CCHFV transcription occurs equally efficient in cells with DM, SM and control. Viruses interfering with microtubule dynamics as well as the use of microtubules in the early steps of a virus life cycle is not unique and have been demonstrated for several viruses, including other members of the *Bunyaviridae* (Dohner and Sodeik, 2005; Elliott and O'Hare, 1998; Jouvenet et al., 2004; Ramanathan and Jonsson, 2008; Ruthel et al., 2005; Smith and Helenius, 2004). In contrast, less is know about the involvement of microtubules in viral replication. In this study we found that CCHFV RNA and progeny virus levels were reduced in response to DM but not to SM when cells were analyzed 16 hpi (Figs. 6B and C). Because primary viral transcription was unaffected (Fig. 5C), we hypothesize that drug treatment one to 16 hpi affects CCHFV replication rather than transcription. The role of intact microtubules in CCHFV RNA synthesis, however, was not critical since we only observed a two-fold reduction in RNA levels when cells were analyzed 16 hpi (Fig. 6C). This also suggests that CCHFV may employ alternate cellular structures during replication. In line with this, most recent publications show that New and Old World hantaviruses are impaired in RNA synthesis when actin filaments or microtubules are disrupted (Ramanathan et al., 2007; Ramanathan and Jonsson, 2008). Furthermore, a possible and indirect role of microtubules was demonstrated in hantavirus replication. It was shown that the viral nucleocapsid protein (NP) translocated along microtubules, and when microtubules were disrupted NP became dispersed and resulted in decreased viral RNA levels (Ramanathan et al., 2007; Ramanathan and Jonsson, 2008). Also, the architecture and function of viral factories in Bunyamwera virus (family *Bunyaviridae*, genus *Orthobunyavirus*) assembly and maturation were shown to require intact actin filaments (Fontana et al.,

2008). We have previously shown that actin is important in CCHFV biogenesis and that CCHFV NP, similar to hantavirus Black Creek Canal virus NP, co-immunoprecipitates with actin (Andersson et al., 2004 data; Ravkov et al., 1998). The results in this study indicate a role of microtubules in the replication process of CCHFV; however, whether actin filaments or microtubules have redundant functions or interact directly with the viral replication complex remain to be elucidated.

In contrast to DM, SM resulted in increased RNA synthesis (Fig. 6D). Further investigation revealed that SM specifically enhanced RNA synthesis, a phenomenon also demonstrated for vesicular stomatitis virus *in vitro* (Moyer et al., 1986). Because we were unable to perform CCHFV replication *in vitro*, we cannot say whether tubulin is pivotal in CCHFV replication, nor whether tubulin *per se* enhances replication. However, since SM results in bundles of microtubules rather than increasing tubulin concentration, it is possible that these bundles rather tether and sequester components necessary for virus replication.

CCHFV glycoproteins are synthesized in the ER before they are transported to the Golgi apparatus for posttranslational processing (Bertolotti-Ciarlet et al., 2005). Subsequent maturation occurs by budding in the cisternae of the Golgi apparatus by the interaction of ribonucleoparticles and glycoproteins before virions are released along the secretory pathway (Schmaljohn and Nichol, 2007). Considering the importance of Golgi in CCHFV biogenesis, disruption of Golgi structure or function may be detrimental for CCHFV assembly and maturation (Hoshino et al., 1997; Sandoval et al., 1984; Thyberg and Moskalewski, 1985). Since fragmented Golgi stacks redistribute close to ER exit sites and continue to promote transport of newly synthesized proteins (Cole et al., 1996), it implies that translocation of CCHFV glycoprotein G_N, from ER to Golgi, should be sustained. Accordingly, our results showed that G_N was associated, albeit less efficiently, with drug-induced fragmented or displaced Golgi elements (Fig. 6B). Moreover, if translocation of viral glycoproteins and subsequent assembly in Golgi is operational in cells with DM or SM, the production of progeny virus titers should only be limited by the availability of RNA. Indeed, the ratio of CCHFV RNA to progeny virus was similar in drug treated and control cells, suggesting that microtubules are not pivotal in CCHFV assembly.

In contrast to G_N, CCHFV NP as well as hantavirus NP, do not associate with Golgi (Andersson et al., 2004; Ramanathan et al., 2007; Ramanathan and Jonsson, 2008). Instead hantavirus NP colocalize with the ER–Golgi intermediate compartment (ERGIC) in a time dependent manner by the employment of microtubules and microtubule-associated motors (Ramanathan et al., 2007; Ramanathan and Jonsson, 2008). ERGIC is an independent structure separated from the ER and the Golgi complex and has been proposed to participate in the biogenesis of several members of the *Bunyaviridae* (Jantti et al., 1997; Matsuoka et al., 1991; Novoa et al., 2005; Ramanathan et al., 2007; Ramanathan and Jonsson, 2008; Salanueva et al., 2003). In terms of viral assembly and maturation, tubular shaped bunyavirus factories were demonstrated to build up around the Golgi complex and were shown to harbour all the necessary components for viral replication and assembly (Fontana et al., 2008). Whether CCHFV NP is transported along microtubules to ERGIC and whether tubular virus factories are part of CCHFV assembly and maturation is currently not known.

Because the endogenous secretory pathway from Golgi to the plasma membrane occurs along microtubules (Luini et al., 2008), it seems reasonable that perturbation of microtubules also impede viral egress. Consequently, we observed that both DM and SM affected CCHFV egress and resulted in a significant reduction of extracellular progeny virus levels (Fig. 8). In cells with DM, we also found that virus assembly was affected, suggesting that microtubules are involved in this process. In contrast, in response to SM, progeny viruses accumulated intracellularly. Thus, it seems that microtubules, directly or indirectly, are involved in CCHFV assembly and egress, and when microtubule dynamics are compromised, it mainly affects egress. In addition to poor assembly, egress in the case of DM could simply be that the tracks necessary for the outward transport of CCHFV are absent. In the case of SM, the bundles of stabilized microtubules could either provide a static barrier or perhaps interfere with the recruitment of necessary structures needed to carry on with viral egress.

In summary, our investigations on the role of microtubules in CCHFV biogenesis have revealed that there are both microtubule dependent and microtubule independent steps in the viral life cycle. We found that CCHFV binding and early transcription was microtubule independent while CCHFV internalization, replication and consequently progeny virus production was impaired in cells with DM. Finally, both DM and SM reduced the extracellular levels of CCHFV with DM also interfering with virus assembly.

Presently, the mechanism underlying CCHFV pathogenesis stands far from complete. The results presented here further our understanding of CCHFV virus–host interactions and provide additional information about the replication process of CCHFV. Thus, more detailed investigations in the future may provide adequate information that will be of importance for the development of antiviral targets needed to fight this emerging virus.

Materials and methods

Cell line and virus

CCHFV strain IbAr 10200, originally isolated in Nigeria in 1970 (Andersson et al., 2004; Flick et al., 2003) was used throughout the experiments. Virus stock and virus titers were produced and determined in Vero cells (monkey kidney cells, ATCC CRL-1587) with indirect immunofluorescent assay (IFA) against the CCHFV nucleocapsid protein (NP) as described elsewhere (Andersson et al., 2004). For CCHFV infections, Vero E6 cells (ATCC CRL-1586) were seeded in 24-well plates and infected for 1 h at 37 °C in serum free Dulbecco's modified Eagle's minimal essential medium (DMEM, Invitrogen Corporation, Carlsbad, CA) supplemented with 10 U/ml penicillin, 10 µg/ml streptomycin and 2% Hepes (Invitrogen products). Viral infectious dose corresponded to 1 multiplicity of infection (moi) (2.5×10^5 focus forming units (FFU)/well). One hour post infection (hpi), cell were rinsed and infection was maintained at 37 °C in DMEM supplemented with penicillin, streptomycin and Hepes as described above and 2% foetal calf serum (FCS, Invitrogen). All infections were carried out in a Biosafety Level 4 laboratory.

Antibodies and drugs

Primary antibodies used in this study were polyclonal rabbit anti-CCHFV NP (Andersson et al., 2004), polyclonal rabbit anti-CCHFV G_N (glycoprotein) (Simon et al., 2006), monoclonal mouse anti-GM130 (Golgi) antibody (BD Biosciences, Franklin Lakes, NJ) and a monoclonal mouse anti-α tubulin antibody (Invitrogen). Secondary antibodies used were anti-rabbit fluorescein isothiocyanate (FITC)-conjugated antibody (DAKO, Glostrup, Denmark), anti-rabbit Alexa Fluor 488 and anti-mouse Alexa Fluor 594 antibodies (Molecular Probes, Invitrogen). All antibodies were diluted in PBS with 0.1% Triton-X100 and 0.2% BSA. The commercial antibodies were used and diluted as recommended by the manufacturer. Nocodazole (NOC, a microtubule depolymerizing drug) (De Brabander et al., 1977) and paclitaxel (PAC, a microtubule stabilizing drug) (De Brabander et al., 1981; Schiff and Horwitz, 1980) (Sigma-Aldrich, Saint Louis, MO) stock solutions were prepared in DMSO according to instructions provided by the manufacturer. Further dilution to working stock, 5 µM for NOC and 20 µM for PAC, was done in culture medium.

Quantitative real-time PCR and determination of relative RNA expression

Cells were harvested with TRIzol and mixed with chloroform followed by a short spin to obtain the water phase with RNA. All subsequent steps for RNA isolation were performed with RNeasy Mini Kit (Qiagen GmbH, Hilden, Germany). cDNA was obtained by reverse transcription of purified RNA with random or gene specific primers and Superscript III (Invitrogen). Random primers were used for the assessment of total RNA while CCHFV S segment forward (5′-GCC-ATGATGTATTTGCCTTTGA-3′) or reverse (5′-CCAGTGAGCCATGAG-CATGT-3′) primers were used to separately determine CCHFV m/cRNA and vRNA levels, respectively. Quantitative real-time PCR analyses were performed in an ABI sequence detector 7900 (Applied Biosystems, Foster City, CA) with 40 cycles (95 °C for 15 s and 60 °C for 1 min). For CCHFV real-time PCR, the same primers as above were used. GAPDH was used as endogenous control (forward primer: 5′-CAGCATCGCCCCACTTG-3′; reverse primer: 5′-GAAATCCCATCACCATC-TTCCA-3′). Amplification reactions were performed in triplicates in MicroAmp 96 well plates containing 20 μl SYBR Green Master mix (Applied Biosciences) with 100 nM of each forward and reverse primer, and cDNA. Relative RNA levels were determined either by CCHFV RNA from non-replicating virus (1 h at 4 °C) as reference or RNA levels were calculated relative to control. Relative RNA levels were calculated with ΔΔCt (User bulletin 2, Applied Biosystems, http://www.appliedbiosystems.com) based on the Ct value for each sample. Uninfected control was included in all assays and was always negative for CCHFV RNA.

Determination of progeny virus titers

Harvested progeny virus was serially 10 fold diluted and then titrated on Vero cells in 96-well plates. Twenty-four hours later, cells were fixed in 80% aceton for 15 min and air-dried before plates were probed with anti-CCHFV NP antibody followed by secondary FITC-conjugated antibody. Probing with primary and secondary antibodies was done at 37 °C for 1 h each. Fluorescent foci were counted in a fluorescent microscope enabling calculation of progeny virus titers in FFU/ml.

Immunofluorescence assay

Vero E6 cells were grown on Lab-Tek II chamber slides (Nalge Nunc International, Rochester, NY) and treated with 5 μM NOC or 20 μM PAC for 30 min at 37 °C. At the end of the incubation, slides were fixed in 4% paraformaldehyde for 10 min followed by incubation in ice-cold methanol for 10 min before probed with anti-α-tubulin antibodies followed by secondary Alexa Fluor 594 antibodies. Images were captured with a Hamamatsu digital camera.

For confocal images, Vero E6 cells were drug treated 6 hpi and maintained in the presence of drugs until 24 hpi. At the end of the infection, slides were fixed as described above and probed with primary anti-α-tubulins or anti-GM130 (cis-Golgi) and anti-CCHFV NP or anti-CCHFV G_N antibodies followed by secondary Alexa Fluor 488 and Alexa Fluor 594 antibodies. Incubation with primary and secondary antibodies was performed at 37 °C for 1 h each. DAPI (4′, 6′-diamidino-2-phenylindole) (Sigma-Aldrich, St. Louis, MO) was used to visualize the cell nucleus. For confocal microscope analysis, images were captured using a DAS microscope Leitz DM RB with a Hamamatsu dual mode cooled charged coupled device camera C4880 at 63× magnification.

Confocal analysis

Confocal microscope images were analyzed for the association of CCHFV proteins (NP and G_N) and GM130 using ImageJ (W. S. Rasband, National Institutes of Health, Bethesda, Md., 1997–2004, http://rsb.info.nih.gov/ij/). Acquired images were analyzed as individual green and red channels corresponding to CCHFV NP or G_N staining and GM130, respectively. Background was corrected using the background subtraction function of ImageJ. Manders' overlap coefficient was generated using the Manders' coefficient plug-in (Manders et al., 1993) that is included in the WCIF version of ImageJ (http://www.uhnresearch.ca/facilites/wcif/imagej/), with regions of interest set for the green channel.

CCHFV RNA synthesis over time

To determine CCHFV positive (m/c) and negative (v) sense RNA synthesis in infected Vero E6 cells over time, cells were infected for one, six or 16 h. At the end of each incubation period, cells were harvested, and RNA was isolated, reverse transcribed and quantified with real-time PCR, as described above.

Microtubule perturbation and CCHFV infection

First we investigated the kinetic of microtubule depolymerization and stabilization in Vero E6 cells. For this, cells were incubated with 5 μM NOC or 20 μM PAC for 30 min at 37 °C, fixed and then stained for α-tubulins before cells were studied under the microscope. To assess drug reversion, cells were first drug treated for 1 h at 37 °C and then rinsed free of drugs. Cells were maintained for an additional 30 min before fixed and stained for α-tubulins.

Next, Vero E6 cells were seeded and grown confluent in 24-well plates and treated with NOC or PAC for 1 h at 37 °C. CCHFV was then allowed to adsorb and bind to the cells for 1 h at 4 °C in the presence of the drugs. At the end of adsorption, unbound virus was removed by washing and cells were harvested with TRIzol (Invitrogen). RNA was isolated, reverse transcribed and quantified with real-time PCR, as described above. To determine CCHFV internalization in the presence of NOC and PAC, Vero E6 cells were pretreated with the drugs (1 h at 37 °C) followed by CCHFV adsorption for 1 h at 4 °C. Internalization was then allowed by a temperature shift to 37 °C for 1 h before cells were rinsed and washed in low pH buffer for 1 min at room temperature to inactive non-internalized virus. Thereafter, cells were rinsed and maintained until 24 hpi before cells were harvested and subjected to Western blot analysis. (Shortly, cell lysates were resolved in 10% Tris–glycine polyacrylamide gel and transferred onto a nitrocellulose membrane. After blocking in non-fat dry-milk, membranes were incubated with primary anti-NP and anti-calnexin antibodies followed by secondary HRP-conjugated antibodies.)

To investigate the effect of microtubule perturbation in prolonged NOC or PAC treatments, Vero E6 cells were sometimes pretreated before infection or drug treated post infection. Detailed illustration of the experiment set-ups are depicted in association to each figure. In infections up to 6 h, only CCHFV RNA levels were determined since neither protein expression or progeny virus could be detected at this time point. For infections exceeding 6 h, RNA or progeny virus levels were used to determine infection efficiency.

Finally, to determine the effect of NOC and PAC in CCHFV egress, Vero E6 cells were drug treated 24 hpi and maintained for 1 h in the presence of drugs before extra- and intracellular progeny virus was collected. Thereafter, cells were rinsed free of drugs to allow for drug reversion and infection was resumed for an additional hour before extra- and intracellular progeny virus was collected and titrated.

Determination of cell viability in response to drug treatment

Measurement of lactate dehydrogenase (LDH) leakage was used to demonstrate potential cell membrane damage. To evaluate the toxicity of NOC and PAC, Vero E6 cells were maintained for 24 h in the presence of drugs before supernatants were harvested and

assayed for LDH according to instructions provided by the manufacturer (CytoTox 96 Non-Radioactive Cytotoxicity Assay, Promega Corporation, Madison, WI).

Statistical analyses

Student's *t*-test was used for the calculation of significant differences between control and drug treated cells. A p-value < 0.05 was considered significant.

Acknowledgments

We thank Mattias Mild for fruitful discussions and valuable comments on the manuscript and Daniel Palm for help with setting up the quantitative real-time PCR. This work was supported by grants from the Swedish Medicine Council (To A.M, K2007-56X-20349-01-3).

References

Andersson, I., Simon, M., Lundkvist, A., Nilsson, M., Holmstrom, A., Elgh, F., Mirazimi, A., 2004. Role of actin filaments in targeting of Crimean Congo hemorrhagic fever virus nucleocapsid protein to perinuclear regions of mammalian cells. J. Med. Virol. 72 (1), 83–93.

Banes, A.J., Coleman, P.H., 1980. La crosse virus production and export have a colchicine-sensitive step. Cell. Biol. Int. Rep. 4 (12), 1117–1123.

Bertolotti-Ciarlet, A., Smith, J., Strecker, K., Paragas, J., Altamura, L.A., McFalls, J.M., Frias-Staheli, N., Garcia-Sastre, A., Schmaljohn, C.S., Doms, R.W., 2005. Cellular localization and antigenic characterization of Crimean-Congo hemorrhagic fever virus glycoproteins. J. Virol. 79 (10), 6152–6161.

Chu, J.J., Ng, M.L., 2004. Infectious entry of West Nile virus occurs through a clathrin-mediated endocytic pathway. J. Virol. 78 (19), 10543–10555.

Cole, N.B., Sciaky, N., Marotta, A., Song, J., Lippincott-Schwartz, J., 1996. Golgi dispersal during microtubule disruption: regeneration of Golgi stacks at peripheral endoplasmic reticulum exit sites. Mol. Biol. Cell. 7 (4), 631–650.

De, B.P., Burdsall, A.L., Banerjee, A.K., 1993. Role of cellular actin in human parainfluenza virus type 3 genome transcription. J. Biol. Chem. 268 (8), 5703–5710.

De Brabander, M., De May, J., Joniau, M., Geuens, G., 1977. Ultrastructural immunocytochemical distribution of tubulin in cultured cells treated with microtubule inhibitors. Cell. Biol. Int. Rep. 1 (2), 177–183.

De Brabander, M., Geuens, G., Nuydens, R., Willebrords, R., De Mey, J., 1981. Taxol induces the assembly of free microtubules in living cells and blocks the organizing capacity of the centrosomes and kinetochores. Proc. Natl. Acad. Sci. U. S. A. 78 (9), 5608–5612.

Dohner, K., Sodeik, B., 2005. The role of the cytoskeleton during viral infection. Curr. Top. Microbiol. Immunol. 285, 67–108.

Dohner, K., Wolfstein, A., Prank, U., Echeverri, C., Dujardin, D., Vallee, R., Sodeik, B., 2002. Function of dynein and dynactin in herpes simplex virus capsid transport. Mol. Biol. Cell. 13 (8), 2795–2809.

Elliott, G., O'Hare, P., 1998. Herpes simplex virus type 1 tegument protein VP22 induces the stabilization and hyperacetylation of microtubules. J. Virol. 72 (8), 6448–6455.

Ergonul, O., 2006. Crimean-Congo haemorrhagic fever. Lancet, Infect. Dis. 6 (4), 203–214.

Flick, R., Flick, K., Feldmann, H., Elgh, F., 2003. Reverse genetics for Crimean-Congo hemorrhagic fever virus. J. Virol. 77 (10), 5997–6006.

Fontana, J., Lopez-Montero, N., Elliott, R.M., Fernandez, J.J., Risco, C., 2008. The unique architecture of Bunyamwera virus factories around the Golgi complex. Cell. Microbiol.

Funk, A., Mhamdi, M., Lin, L., Will, H., Sirma, H., 2004. Itinerary of hepatitis B viruses: delineation of restriction points critical for infectious entry. J. Virol. 78 (15), 8289–8300.

Gavrilovskaya, I.N., Shepley, M., Shaw, R., Ginsberg, M.H., Mackow, E.R., 1998. beta3 Integrins mediate the cellular entry of hantaviruses that cause respiratory failure. Proc. Natl. Acad. Sci. U. S. A. 95 (12), 7074–7079.

Gubler, D.J., Reiter, P., Ebi, K.L., Yap, W., Nasci, R., Patz, J.A., 2001. Climate variability and change in the United States: potential impacts on vector- and rodent-borne diseases. Environ. Health Perspect. 109 (Suppl 2), 223–233.

Gupta, S., De, B.P., Drazba, J.A., Banerjee, A.K., 1998. Involvement of actin microfilaments in the replication of human parainfluenza virus type 3. J. Virol. 72 (4), 2655–2662.

Hoshino, H., Tamaki, A., Yagura, T., 1997. Process of dispersion and fragmentation of Golgi complex by microtubule bundles formed in taxol treated HeLa cells. Cell. Struct. Funct. 22 (3), 325–334.

Igakura, T., Stinchcombe, J.C., Goon, P.K., Taylor, G.P., Weber, J.N., Griffiths, G.M., Tanaka, Y., Osame, M., Bangham, C.R., 2003. Spread of HTLV-I between lymphocytes by virus-induced polarization of the cytoskeleton. Science 299 (5613), 1713–1716.

Jantti, J., Hilden, P., Ronka, H., Makiranta, V., Keranen, S., Kuismanen, E., 1997. Immunocytochemical analysis of Uukuniemi virus budding compartments: role of the intermediate compartment and the Golgi stack in virus maturation. J. Virol. 71 (2), 1162–1172.

Jin, M., Park, J., Lee, S., Park, B., Shin, J., Song, K.J., Ahn, T.I., Hwang, S.Y., Ahn, B.Y., Ahn, K., 2002. Hantaan virus enters cells by clathrin-dependent receptor-mediated endocytosis. Virology 294 (1), 60–69.

Jouvenet, N., Wileman, T., 2005. African swine fever virus infection disrupts centrosome assembly and function. J. Gen. Virol. 86 (Pt 3), 589–594.

Jouvenet, N., Monaghan, P., Way, M., Wileman, T., 2004. Transport of African swine fever virus from assembly sites to the plasma membrane is dependent on microtubules and conventional kinesin. J. Virol. 78 (15), 7990–8001.

Kuhn, M., Desloges, N., Rahaus, M., Wolff, M.H., 2005. Varicella-zoster virus infection influences expression and organization of actin and alpha-tubulin but does not affect lamin A and vimentin. Intervirology 48 (5), 312–320.

Lakadamyali, M., Rust, M.J., Babcock, H.P., Zhuang, X., 2003. Visualizing infection of individual influenza viruses. Proc. Natl. Acad. Sci. U. S. A. 100 (16), 9280–9285.

Luby-Phelps, K., 2000. Cytoarchitecture and physical properties of cytoplasm: volume, viscosity, diffusion, intracellular surface area. Int. Rev. Cytol. 192, 189–221.

Luini, A., Mironov, A.A., Polishchuk, E.V., Polishchuk, R.S., 2008. Morphogenesis of post-Golgi transport carriers. Histochem. Cell. Biol. 129 (2), 153–161.

Mallardo, M., Schleich, S., Krijnse Locker, J., 2001. Microtubule-dependent organization of vaccinia virus core-derived early mRNAs into distinct cytoplasmic structures. Mol. Biol. Cell. 12 (12), 3875–3891.

Manders, E.M.M., Verbeek, F.J., Aten, J.A., 1993. Measurement of co-localisation of objects in dual-colour confocal images. J. Microsc. 169, 375–382.

Matsuoka, Y., Chen, S.Y., Compans, R.W., 1991. Bunyavirus protein transport and assembly. Curr. Top Microbiol. Immunol. 169, 161–179.

McDonald, D., Vodicka, M.A., Lucero, G., Svitkina, T.M., Borisy, G.G., Emerman, M., Hope, T.J., 2002. Visualization of the intracellular behavior of HIV in living cells. J. Cell. Biol. 159 (3), 441–452.

Moyer, S.A., Baker, S.C., Lessard, J.L., 1986. Tubulin: a factor necessary for the synthesis of both Sendai virus and vesicular stomatitis virus RNAs. Proc. Natl. Acad. Sci. U. S. A. 83 (15), 5405–5409.

Naghavi, M.H., Valente, S., Hatziioannou, T., de Los Santos, K., Wen, Y., Mott, C., Gundersen, G.G., Goff, S.P., 2007. Moesin regulates stable microtubule formation and limits retroviral infection in cultured cells. EMBO J. 26 (1), 41–52.

Newsome, T.P., Scaplehorn, N., Way, M., 2004. SRC mediates a switch from microtubule- to actin-based motility of vaccinia virus. Science 306 (5693), 124–129.

Novoa, R.R., Calderita, G., Arranz, R., Fontana, J., Granzow, H., Risco, C., 2005. Virus factories: associations of cell organelles for viral replication and morphogenesis. Biol. Cell. 97 (2), 147–172.

Pelkmans, L., Kartenbeck, J., Helenius, A., 2001. Caveolar endocytosis of simian virus 40 reveals a new two-step vesicular-transport pathway to the ER. Nat. Cell. Biol. 3 (5), 473–483.

Ploubidou, A., Moreau, V., Ashman, K., Reckmann, I., Gonzalez, C., Way, M., 2000. Vaccinia virus infection disrupts microtubule organization and centrosome function. EMBO J. 19 (15), 3932–3944.

Ramanathan, H.N., Chung, D.H., Plane, S.J., Sztul, E., Chu, Y.K., Guttieri, M.C., McDowell, M., Ali, G., Jonsson, C.B., 2007. Dynein-dependent transport of the Hantaan virus nucleocapsid protein to the endoplasmic reticulum–Golgi intermediate compartment. J. Virol. 81 (16), 8634–8647.

Ramanathan, H.N., Jonsson, C.B., 2008. New and Old World hantaviruses differentially utilize host cytoskeletal components during their life cycles. Virology.

Ravkov, E.V., Nichol, S.T., Peters, C.J., Compans, R.W., 1998. Role of actin microfilaments in Black Creek Canal virus morphogenesis. J. Virol. 72 (4), 2865–2870.

Rietdorf, J., Ploubidou, A., Reckmann, I., Holmstrom, A., Frischknecht, F., Zettl, M., Zimmermann, T., Way, M., 2001. Kinesin-dependent movement on microtubules precedes actin-based motility of vaccinia virus. Nat. Cell. Biol. 3 (11), 992–1000.

Ruthel, G., Demmin, G.L., Kallstrom, G., Javid, M.P., Badie, S.S., Will, A.B., Nelle, T., Schokman, R., Nguyen, T.L., Carra, J.H., Bavari, S., Aman, M.J., 2005. Association of ebola virus matrix protein VP40 with microtubules. J. Virol. 79 (8), 4709–4719.

Salanueva, I.J., Novoa, R.R., Cabezas, P., Lopez-Iglesias, C., Carrascosa, J.L., Elliott, R.M., Risco, C., 2003. Polymorphism and structural maturation of Bunyamwera virus in Golgi and post-Golgi compartments. J. Virol. 77 (2), 1368–1381.

Sandoval, I.V., Bonifacino, J.S., Klausner, R.D., Henkart, M., Wehland, J., 1984. Role of microtubules in the organization and localization of the Golgi apparatus. J. Cell. Biol. 99 (1 Pt 2), 113s–118s.

Schiff, P.B., Horwitz, S.B., 1980. Taxol stabilizes microtubules in mouse fibroblast cells. Proc. Natl. Acad. Sci. U. S. A. 77 (3), 1561–1565.

Schmaljohn, C.S., Nichol, S.T., 2007. Bunyaviridae, 5th ed. Lippincott Williams and Wilkins, Philadelphia, PA.

Simon, M., Falk, K.I., Lundkvist, A., Mirazimi, A., 2006. Exogenous nitric oxide inhibits Crimean Congo hemorrhagic fever virus. Virus. Res. 120 (1–2), 184–190.

Simpson-Holley, M., Ellis, D., Fisher, D., Elton, D., McCauley, J., Digard, P., 2002. A functional link between the actin cytoskeleton and lipid rafts during budding of filamentous influenza virions. Virology 301 (2), 212–225.

Smith, G.A., Enquist, L.W., 2002. Break ins and break outs: viral interactions with the cytoskeleton of mammalian cells. Annu. Rev. Cell. Dev. Biol. 18, 135–161.

Smith, A.E., Helenius, A., 2004. How viruses enter animal cells. Science 304 (5668), 237–242.

Sodeik, B., Ebersold, M.W., Helenius, A., 1997. Microtubule-mediated transport of incoming herpes simplex virus 1 capsids to the nucleus. J. Cell. Biol. 136 (5), 1007–1021.

Suikkanen, S., Aaltonen, T., Nevalainen, M., Valilehto, O., Lindholm, L., Vuento, M., Vihinen-Ranta, M., 2003. Exploitation of microtubule cytoskeleton and dynein during parvoviral traffic toward the nucleus. J. Virol. 77 (19), 10270–10279.

Suomalainen, M., Nakano, M.Y., Keller, S., Boucke, K., Stidwill, R.P., Greber, U.F., 1999. Microtubule-dependent plus- and minus end-directed motilities are competing processes for nuclear targeting of adenovirus. J. Cell. Biol. 144 (4), 657–672.

Swanepoel, R., Shepherd, A.J., Leman, P.A., Shepherd, S.P., McGillivray, G.M., Erasmus, M.J., Searle, L.A., Gill, D.E., 1987. Epidemiologic and clinical features of Crimean-Congo hemorrhagic fever in southern Africa. Am. J. Trop. Med. Hyg. 36 (1), 120–132.

Thyberg, J., Moskalewski, S., 1985. Microtubules and the organization of the Golgi complex. Exp. Cell. Res. 159 (1), 1–16.

Whitehouse, C.A., 2004. Crimean-Congo hemorrhagic fever. Antiviral. Res. 64 (3), 145–160.

Yonezawa, A., Cavrois, M., Greene, W.C., 2005. Studies of Ebola virus glycoprotein-mediated entry and fusion by using pseudotyped human immunodeficiency virus type 1 virions: involvement of cytoskeletal proteins and enhancement by tumor necrosis factor alpha. J. Virol. 79 (2), 918–926.

Zeller, H.G., Cornet, J.P., Camicas, J.L., 1994. Experimental transmission of Crimean-Congo hemorrhagic fever virus by west African wild ground-feeding birds to *Hyalomma marginatum rufipes* ticks. Am. J. Trop. Med. Hyg. 50 (6), 676–681.